

Molecular gas freeze-out in the pre-stellar core L1689B

M.P. Redman¹, J.M.C. Rawlings¹, D.J. Nutter², D. Ward-Thompson², D.A. Williams¹

¹ *Department of Physics & Astronomy, University College London, Gower Street, London WC1E 6BT, UK.*

² *Department of Physics and Astronomy, Cardiff University, PO Box 913, Cardiff CF2 3YB, UK.*

23 November 2018

ABSTRACT

$C^{17}O$ $J = 2 \rightarrow 1$ observations have been carried out towards the pre-stellar core L1689B. By comparing the relative strengths of the hyperfine components of this line, the emission is shown to be optically thin. This allows accurate CO column densities to be determined and, for reference, this calculation is described in detail. The hydrogen column densities that these measurements imply are substantially smaller than those calculated from SCUBA dust emission data. Furthermore, the $C^{17}O$ $J = 2 \rightarrow 1$ column densities are approximately constant across L1689B whereas the SCUBA column densities are peaked towards the centre. The most likely explanation is that CO is depleted from the central regions of L1689B. Simple models of pre-stellar cores with an inner depleted region are compared with the results. This enables the magnitude of the CO depletion to be quantified and also allows the spatial extent of the freeze-out to be firmly established. We estimate that within about 5000 AU of the centre of L1689B, over 90% of the CO has frozen onto grains. This level of depletion can only be achieved after a duration that is at least comparable to the free-fall timescale.

Key words: radiative transfer - ISM: globules - ISM: individual: L1689B - stars: formation - stars:pre-main-sequence - submillimetre

1 INTRODUCTION

Molecular line profiles from pre-stellar and protostellar objects potentially offer the best opportunity to extract dynamical information about the collapse process that leads to the formation of stars. However, it is becoming clear that the interpretation of these line profiles can be fraught with difficulty. Rawlings & Yates (2001) used a self-consistent chemical and dynamical model of collapsing star-forming cores to explore the effects of abundance variations. They showed that the line profiles can be very sensitive to the assumed values of the free parameters in the chemical models. The depletion of molecular species due to freeze-out can have a profound influence on the line profiles. Accurate abundances are required deep within these cores in order that any freeze-out is characterised properly.

The widely used tracer of molecular hydrogen, CO, is so abundant that, in the cold dark clouds in which stars are forming, it has a large optical depth and thus cannot trace the densest material. Very rare CO isotopomers are therefore used and in order of decreasing abundance these are ^{13}CO , $C^{18}O$, $C^{17}O$, $^{13}C^{18}O$ and $^{13}C^{17}O$, recently discovered by Bensch et al. (2001) toward the ρ Ophiuchi molecular cloud. Measuring abundances is not straightforward however because even some of the rare isotopes are mildly optically thick and the very rare isotopes can require impractically large integration times. $C^{18}O$ is often selected as a result of

these conflicting demands but the analysis can be complicated by the lack of an optical depth estimate. In contrast, $C^{17}O$ is slightly less abundant than $C^{18}O$ and has a complex hyperfine structure revealed in several distinct line components. For a well detected line the hyperfine structure can be used to identify whether optical depth effects are present and hence abundances can confidently be calculated.

Of course, in order to calculate hydrogen column densities, abundance ratios between the different isotopomers are required. Bensch et al. (2001) demonstrated how by using several different isotopes of CO, the optical depths could be cross-checked and the abundance ratios measured. Effects such as isotope-selective photo-dissociation and chemical fractionation can be important in translucent clouds but are not thought to be significant in the cold dense environments considered here (Bensch et al. 2001).

Dust emission measurements can be used to calculate dust column densities and using a dust to gas ratio, a second estimate for the column density of hydrogen can be made. If this exceeds the hydrogen column density as traced by CO then it is possible that the CO is depleted from the gas-phase. The most probable reason for this is that the CO has frozen onto the surfaces of grains. Gibb & Little (1998) find CO abundances reduced by a factor of at least 10 towards the HH24-26 molecular cloud core by this method. They also carefully consider alternative explanations that do not require abundance differences such as optical depth

and beam filling effects and show them to be unlikely. Recently Bergin et al. (2002) have found that not only CO but N_2H^+ is depleted in the Bok globule B68. This raises the possibility that in some cores there will be very few available infall tracers. Two very recent papers have investigated CO depletion. Bacmann et al. (2002) have investigated seven pre-stellar cores and find CO to be underabundant by factors of 4-15 amongst the cores. Jørgensen et al. (2002) modelled 18 pre-stellar cores and found that the class 0 sources in their sample are depleted in CO by an order of magnitude.

L1689B is a pre-stellar core located in Ophiuchus. Gregersen & Evans (2000) have observed L1689B in the lines of $\text{HCO}^+ J = 3 \rightarrow 2$ and $\text{H}^{13}\text{CO}^+ J = 3 \rightarrow 2$. Their multipoint data seemed to indicate that the $\text{HCO}^+ J = 3 \rightarrow 2$ emission was double-peaked and blue-skewed, indicative of infall. This is supported by the single point CS $J = 2 \rightarrow 1$ observations by Lee et al. (1999) which show a clear blue-peak asymmetry. Jessop & Ward-Thompson (2001) observed L1689B in C^{18}O and although they did not have optical depth measurements and thus column densities for C^{18}O they explored the dust density and temperature parameter space and argued that the CO has to be depleted in order to be compatible with the continuum data.

In this paper, observations of the rare C^{17}O isotope are presented and column densities derived and analysed in an attempt to quantify any depletion that is taking place. These data are discussed in terms of current models for pre-stellar cores in general and L1689B in particular.

2 OBSERVATIONS

The observations were carried out at the James Clark Maxwell Telescope (JCMT), Mauna Kea, Hawaii on the night of 2001 August 19. The $\text{C}^{17}\text{O } J = 2 \rightarrow 1$ (224.714368 GHz) rotational transition was observed using the heterodyne receiver RxA3. The JCMT half-power beam width (HPBW) is 19 arcsec at these frequencies. Typical system temperatures were 325 K. Five pointings at 20 arcsecond offsets at (-40,0), (-20,0), (0,0), (20,0), (40,0) were obtained for $\text{C}^{17}\text{O } J = 2 \rightarrow 1$, centred at the epoch 1950 position (16:31:46.90, -24:31:55.98). Jessop & Ward-Thompson (2001) and Gregersen & Evans (2000) used a pointing position of (16:31:46.98, -24:31:45.00) while Lee et al. (1999) used a pointing position of (16:31:43.6,-24:31:40). The data were reduced in the standard manner using SPECX and the resulting spectra are displayed in Figure 1

3 RESULTS

Due to the spin of the ^{17}O nucleus, $\text{C}^{17}\text{O } J = 2 \rightarrow 1$ is composed of nine hyperfine components. Figure 2 depicts these components and their relative strengths (from the tabulation of Ladd et al. 1998). The hyperfine components are shown with very narrow line widths and also with a broadening of 0.35 km s^{-1} to illustrate the typical line shape that can be expected to be observed in cold quiescent cores. Since the stronger components will be affected relatively more by non-negligible optical depths, the shape of the blended line can be used to verify that the emission is optically thin in this line and transition. Figure 3 depicts an overlay of the

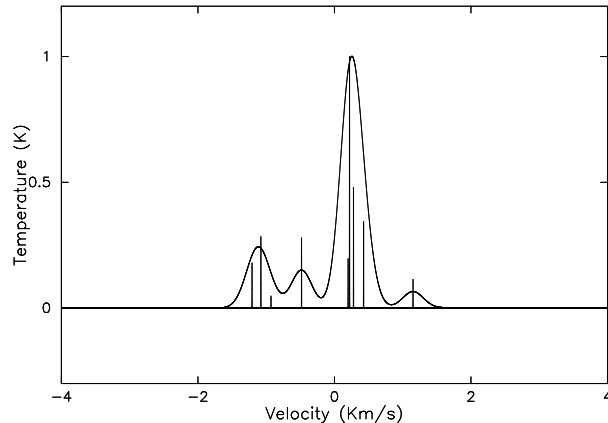


Figure 2. Fine structure of the $\text{C}^{17}\text{O } J = 2 \rightarrow 1$ transition. The narrow spikes illustrate the relative velocities and strengths of the hyperfine components. The curve is these components smoothed with a gaussian profile with $\sigma = 0.15 \text{ km s}^{-1}$. Both the spikes and the smoothed curve are normalised to their peak intensities

data from the central position of L1689B with the expected optically thin line shape. We can conclude from the close fit that the line does not display any significant saturation effects and is thus of low optical depth. A detailed fit, using the HFS routine in the CLASS software package gives optical depths in the range 0.5 – 1.5. For such low optical depths, the actual value obtained from the software should be treated with some caution as the deviations from an optically thin line shape are very small (for example, the fit in Fig. 3 is for very low optical depth) and likely to be strongly affected by the noise. In our later analysis, we adopt an optical depth of ~ 0.7 for all positions because this is consistent with other recent measurements (N.J. Evans II, 2002 private communication). The results of the fit are given in Table 1 which also lists the line centre, line widths and optical depths obtained. The net broadening (due to turbulent and instrumental broadening), $V_{\text{broad}} \simeq 0.37 \text{ km s}^{-1}$. This is smaller than the C^{18}O line width than measured by Jessop & Ward-Thompson (2001) who find $V_{\text{FWHM}} \simeq 0.6 - 0.8 \text{ km s}^{-1}$ for their singly peaked and gaussian line profiles (though as discussed below, this line is actually optically thick).

3.1 CO column densities

If it is assumed that the optical depth is small, local thermodynamic equilibrium holds, and the excitation temperature $T_{\text{ex}} \gg T_{\text{cmb}}$ then the total column density of a species is given by

$$N_{\text{tot}} = \frac{3k}{8\pi^3\nu} \frac{Q(T_{\text{ex}})}{\mu^2 S} \exp\left(\frac{E_u}{kT_{\text{ex}}}\right) \int T_{\text{mb}} dV. \quad (1)$$

where $\int T_{\text{mb}} dV \simeq T_{\text{A}}^* \Delta V / \eta_{\text{B}}$, the integrated line intensity. If the integrated line strength is measured in km s^{-1} , frequency in GHz, μ in debye ($1 \text{ debye} = (1/3) \times 10^{-29} \text{ C m}$) and if an SI to CGS conversion factor of $4\pi\epsilon_0$ is used then the column density is

$$N_{\text{tot}} = 1.67 \times 10^{14} \text{ cm}^{-2} \frac{Q(T_{\text{ex}})}{\nu \mu^2 S} \times \exp\left(\frac{E_u}{kT_{\text{ex}}}\right) \int T_{\text{mb}} dV. \quad (2)$$

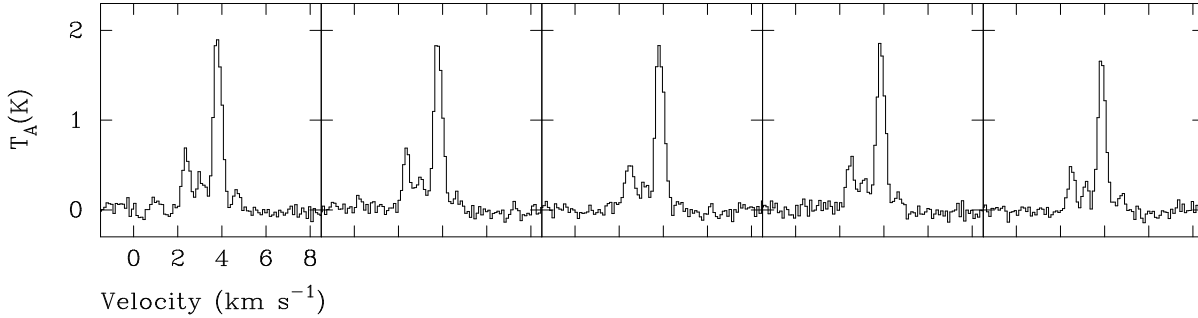


Figure 1. $C^{17}O$ $J = 2 \rightarrow 1$ line profiles from offset positions of (from left to right) $-40''$, $-20''$, $0''$, $20''$, $40''$

Offset	Line centre (km s^{-1})	Line width (km s^{-1})	$\tau_{C^{17}O}$	$\int T_A^* dV$ K km s^{-1}	$N_{C^{17}O}$ cm^{-2}	N_{tot} cm^{-2}
$-40''$	3.577 ± 0.004	0.393 ± 0.012	0.673 ± 0.240	1.45	1.0×10^{15}	1.3×10^{22}
$-20''$	3.592 ± 0.004	0.378 ± 0.013	1.028 ± 0.242	1.43	9.9×10^{14}	1.3×10^{22}
$0''$	3.526 ± 0.004	0.370 ± 0.012	1.346 ± 0.262	1.35	9.3×10^{14}	1.2×10^{22}
$20''$	3.608 ± 0.004	0.346 ± 0.013	0.526 ± 0.278	1.34	9.3×10^{14}	1.2×10^{22}
$40''$	3.537 ± 0.004	0.356 ± 0.011	1.462 ± 0.273	1.09	7.5×10^{14}	9.9×10^{21}

Table 1. Optical depths, $C^{17}O$ column densities and estimated total column densities for each offset position.

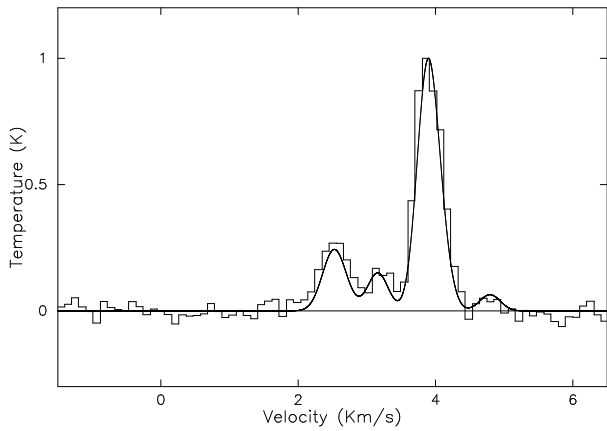


Figure 3. $C^{17}O$ $J = 2 \rightarrow 1$ data and expected line shape if the emission is optically thin with a turbulent velocity dispersion of 0.15 km s^{-1} as in Figure 2 offset to 3.64 km s^{-1} . Both the data and the expected line shape are normalised to their peak intensities

The excitation temperature is taken to be 12K, as inferred by Jessop & Ward-Thompson (2001). The rotational energy levels are assumed to be thermalized at T_{ex} and the partition function $Q(T_{\text{ex}})$ for each species is evaluated by interpolating between values obtained from the JPL molecular line database (Pickett et al. 1998) and these are also listed in Table 2. Calculating a hydrogen column density from the $C^{17}O$ emission requires knowledge of three conversion factors: the H_2/CO abundance ratio, which we take to be 3700 (Lacy et al. 1994); the oxygen isotope ratios $^{16}O/^{18}O$, taken to be 560 (Wilson & Rood 1994) and $^{18}O/^{17}O$, taken to be 3.65 (Ladd et al. 1998; Penzias 1981). The final conversion factor from $C^{17}O$ to H_2 is 7.56×10^6 .

Column densities are also calculated using archive $C^{18}O$ $J = 2 \rightarrow 1$ data of Jessop & Ward-Thompson (2001).

Parameter	$C^{17}O$ $J = 2 \rightarrow 1$	$C^{18}O$ $J = 2 \rightarrow 1$
ν (GHz)	224.714	219.560
E_u (K)	16.177	15.8058
μ (Debye)	0.11034	0.11079
S	2	2
$Q(12.0 \text{ K})$	4.80	4.93

Table 2. Molecular data for $C^{17}O$ and $C^{18}O$.

This is possible since the $C^{17}O$ $J = 2 \rightarrow 1$ line is optically thin and so the optical depth of the $C^{18}O$ $J = 2 \rightarrow 1$ line can be calculated. Ladd et al. (1998) show that simply using the ratio of the peaks in these lines to calculate the optical depth is unsuitable. This is because the closely spaced fine structure of the $C^{17}O$ $J = 2 \rightarrow 1$ line means that the peak in this transition is very sensitive to the turbulent velocity. The integrated intensities are much more robust and the ratio of these are compared with figure 1 of Ladd et al. (1998) to infer that the optical depth in the $C^{18}O$ $J = 2 \rightarrow 1$ line is $\tau_{C^{18}O} \gtrsim 2$. When the optical depth is moderate as in this case, Eqn (1) multiplied by a correction factor of $\tau/(1 - \exp -\tau)$ can be used to calculate column density.

The column densities derived from the two lines are plotted as a function of offset in Figure 4. The agreement is excellent and both datasets show that the column density is remarkably flat across the face of the core.

3.2 Dust column densities

Evans et al. (2001) obtained SCUBA maps of L1689B and carried out a detailed radiative transfer analysis of the dust emission which enable them to place constraints on the temperature and density distribution in the envelope. The gas density distribution was well fitted by a Bonner-Ebert sphere with a central density of $n_c = 1 \times 10^6 \text{ cm}^{-3}$ and outer

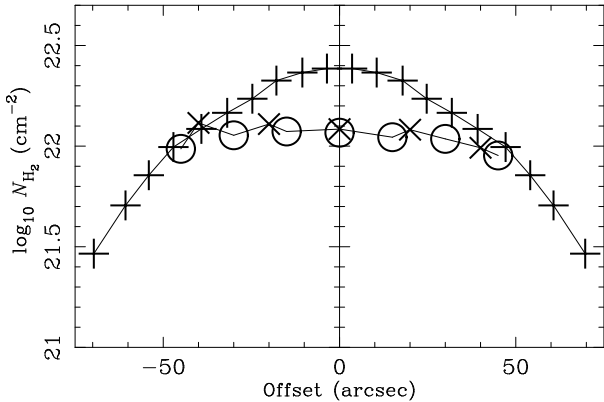


Figure 4. Column densities across L1689B, measured using the $C^{17}O J = 2 \rightarrow 1$ transition (crosses), $C^{18}O$ data of Jessop & Ward-Thompson (2001) (circles) and from SCUBA 850 μm radial profile fits of Evans et al. (2001) (pluses). The sizes of the symbols may be taken as a rough indication of the observational error.

radius of 3×10^4 AU. The dust opacities used were from Ossenkopf & Henning (1994). Using the azimuthally averaged results of Evans et al. (2001), and their dust opacity, we calculate dust column densities, based on an assumed gas to dust mass ratio of 100 according to the usual formula

$$N = S_{850} / [\Omega \kappa_{850\mu\text{m}} m_{\text{H}} B_{850}(T)] \quad (3)$$

where $S_{850} = 0.7$ Jy is the flux at 850 microns within a $33''$ beam, Ω is the solid angle subtended by the beam, $\kappa_{850\mu\text{m}} = 0.018 \text{ cm}^2 \text{ g}^{-1}$ is the dust opacity, $\mu = 2.2$ is the mean molecular weight, m_{H} is the mass of hydrogen and $B_{850\mu\text{m}}(T)$ is the Planck function at $T = 12$ K. The dust column densities are plotted in Figure 4 and are consistent with those obtained by Bacmann et al. (2000, 2002) (who use a different opacity to calculate their column densities) and Ward-Thompson et al. (2002).

3.3 Depletion of CO

It is clear from Figure 4 that the two independent techniques for measuring the column density produce results that differ both in magnitude and distribution. As inferred by the above discussions, the exact normalisations of the curves in Figure 4 are subject to variation depending on the adopted values of dust opacity, isotopic ratios and molecular abundances. The most important aspect of Figure 4 is the flatness of the column density plot from CO compared with the centrally peaked dust measurements. This strongly indicates that depletion is occurring because the column density should rise for positions that approach the dense centre of the object. The most likely reason for this depletion is that the CO has frozen to the surface of the dust grains deep within the core. The best fit dust models of Evans et al. (2001) have a dust temperature profile that drops from ~ 12 K at the edge of this pre-stellar core down to a temperature of ~ 7 K at the centre. The combination of the higher gas density and the lower dust temperature is the likely reason for a substantial freeze-out of CO in the central regions of L1689B. An alternative explanation for these data is that the CO lies along the line of sight and is not actually part of the L1689B core. This can be ruled out since

this would require the core to be completely depleted of CO in order that the column density remains roughly constant across the face of it.

Jessop & Ward-Thompson (2001) compared their $C^{18}O J = 2 \rightarrow 1$ data with earlier mm continuum data of André et al. (1996). Using a model for L1689B with power law profiles for the density, temperature and CO abundance, they explored the parameter space that would be consistent with both datasets. They conclude that the CO could be depleted by up to 95% but they did not have an optical depth measurement for their $C^{18}O$ data. In contrast, our results indicate that the ratio of the column densities towards the centre is only around a factor of 3 or so. Of course, the CO is unlikely to be uniformly depleted and this factor of 3 represents the column depletion. The local depletion is likely to be much higher. This can be investigated by plotting the column densities that result from models where the radial density profile, abundance and temperature are all varied. To illustrate this in a very simple case, we use a constant temperature model and vary the abundance such that interior to a certain radius R_{freeze} the CO is depleted by a factor 0.95 due to freeze-out. Instead of using the Bonner-Ebert density distributions which are inconvenient to work with, we use the parameters of the fit of Evans et al. (2001) in an equivalent Plummer-like sphere which has a density profile of the form (see, e.g. Whitworth & Ward-Thompson 2001; Whitworth & Bate 2001)

$$\rho(r) = \frac{\rho_0 R_0^2}{(R_0^2 + r^2)} \quad (4)$$

where $\rho_0 = 1.0 \times 10^6 \text{ cm}^{-3}$ is the central density and $R_0 = 750$ AU is an inner radius within which the density is approximately ρ_0 . For the purposes here, the difference between the Bonner-Ebert and Plummer density distributions are of little consequence - both approximate $\rho \sim r^{-2}$ in the envelope and are roughly constant close to the centre. Figure 5 shows the column density that results from this simple Plummer sphere model for a range of values of R_{freeze} with the top curve showing the underlying density distribution. Comparison with Figure 4 shows clearly that values of R_{freeze} of about $40'' \equiv 5000$ AU would be able to reproduce the approximately flat CO abundance with a column depletion factor of about the correct degree. One could of course investigate the parameter space fully and include realistic variations in the freeze-out and temperature but we defer that to a later paper.

The close fit of the $C^{17}O J = 2 \rightarrow 1$ lines by a model with only turbulent velocities (i.e. with no infall or outflow) indicates that the CO emitting material is static. In contrast, the $\text{HCO}^+ J = 3 \rightarrow 2$ and $\text{H}^{13}\text{CO}^+ J = 3 \rightarrow 2$ data of Gregersen & Evans (2000) show double peaked line profiles indicating both that the HCO^+ is self-absorbed and that the gas is undergoing bulk gas motions. These emissions are likely to originate from within the denser regions of the core. The flatness of the abundance points across the core measured using $C^{17}O J = 2 \rightarrow 1$ (Figure 4) indicates that the CO is depleted from the central regions. Thus one can picture that L1689B is composed of a dynamical dense core which is depleted in CO but in which HCO^+ is present. This is surrounded by a quiescent surrounding region where both CO and HCO^+ are present.

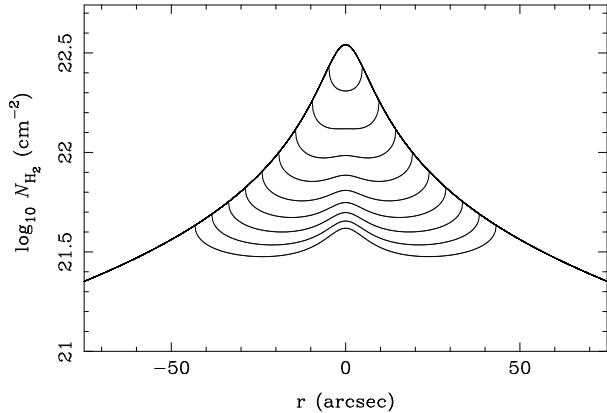


Figure 5. Column densities from a Plummer-like sphere density distribution with a depletion ‘hole’ that extends from the centre to a radius R_{freeze} . The local depletion within the hole is such that only 5% of the CO remains in the gas phase. The upper most curve is with no depletion. The curves below it are for values of R_{freeze} of between 5 and 45 arcseconds. The curves have not been convolved with a telescope beam and hence are more centrally peaked than the observational data.

4 CONCLUSIONS

Rare isotopes of CO have been observed towards the pre-stellar core L1689B. By using the hyperfine structure of C^{17}O $J = 2 \rightarrow 1$ the transition is confirmed to be optically thin and emitted by quiescent gas. This allows an estimate of the total column density as traced by this molecule to be made. A comparison of this value with that inferred by SCUBA dust emission measurements reveal the CO to be depleted in the central regions of this object. The magnitude and extent of the depletion is estimated by comparison with a simple model of a pre-stellar core with an inner depleted region. We estimate that within 5000 AU of the centre of L1689B, around 90% of the CO has frozen onto grains. The dust temperature at this radius is $\simeq 10$ K (from figure 5 of Evans et al. 2001). The sublimation temperature of CO is $\simeq 20$ K so potentially freeze-out could occur in the outer regions of the cloud. In practice of course, the timescale for freeze-out in the low density outer regions is long and freeze-out will occur only in those portions of the cloud with a high local density and low dust temperature.

For the physical parameters of L1689B, the rate of freeze-out of CO is given by (Rawlings et al. 1992)

$$\dot{n}_{\text{CO}} = 4.57 \times 10^4 d_g a^2 T^{1/2} C n_{\text{H}} S_{\text{CO}} m_{\text{CO}} \text{ cm}^{-3} \text{ s}^{-1} \quad (5)$$

where n_{H} and n_{CO} are the hydrogen nucleon and CO densities respectively, $m_{\text{CO}} = 28$ amu is the molecular mass of CO, d_g is the ratio of the number density of grains to CO molecules, a is the grain radius, C is a factor which accounts for electrostatic effects, $S_{\text{CO}} = 1$ is the assumed sticking coefficient for CO. Using $\langle d_g a^2 \rangle \simeq 2.2 \times 10^{-22} \text{ cm}^{-2}$ and $T \sim 10$ K yields

$$\dot{n}_{\text{CO}} = 6.0 \times 10^{-18} n_{\text{H}} n_{\text{CO}} \text{ cm}^{-3} \text{ s}^{-1} \quad (6)$$

Using a value of $n_{\text{H}} = 2.8 \times 10^5 \text{ cm}^{-3}$ for L1689B (Bacmann et al. 2000) we find that in the absence of other CO formation and destruction mechanisms, 90% depletion of CO is achieved after $\sim 43,400$ years. This is approximately half of the nominal free-fall timescale (97,400 years) for the value

of n_{H} quoted above, but we should be aware that the freeze-out timescale is a *lower* limit and would be larger if the sticking coefficient were less than unity, or if (as would seem likely) the cores have condensed from a less dense state. We may therefore conclude that the level of CO depletion may provide a sensitive indicator of the age of cores relative to their free-fall times and that a C^{17}O survey of sources at various (early) stages of evolution could provide a powerful diagnostic of their dynamical status.

ACKNOWLEDGEMENTS

We thank the referee for a prompt report that led to an improved paper. We thank W-F.D. Thi for useful discussions. MPR and DJN are supported by PPARC. We thank the staff of the JCMT for their excellent assistance during the observations. The JCMT is operated by the JAC, Hawaii, on behalf of the UK PPARC, the Netherlands NWO, and the Canadian NRC. We have made use of the JCMT data archive at the CADC, which is operated by the Dominion Astrophysical Observatory for the National Research Council of Canada’s Herzberg Institute of Astrophysics.

REFERENCES

- André P., Ward-Thompson D., Motte F., 1996, *A&A*, 314, 625
 Bacmann A., André P., Puget J. L., et al 2000, *A&A*, 361, 555
 Bacmann A., Lefloch B., Cecarelli C., et al 2002, *A&A*, 389, L6
 Bensch F., Pak I., Wouterloot J. G. A., Klapper G., Winnewisser G., 2001, *ApJ*, 562, L185
 Bergin E. A., Alves J., Huard T. L., Lada C. J., 2002, *ApJ*, In press
 Evans N. J., Rawlings J. M. C., Shirley Y. L., Mundy L. G., 2001, *ApJ*, 557, 193
 Gibb A. G., Little L. T., 1998, *MNRAS*, 295, 299
 Gregersen E. M., Evans N. J., 2000, *ApJ*, 538, 260
 Jessop N. E., Ward-Thompson D., 2001, *MNRAS*, 323, 1025
 Jørgensen J. K., Schöier F.L. van Dishoeck E. F., 2002, *A&A*, in press
 Lacy J. H., Knacke R., Geballe T. R., Tokunaga A. T., 1994, *ApJ*, 428, L69
 Ladd E. F., Fuller G. A., Deane J. R., 1998, *ApJ*, 495, 871
 Lee C. W., Myers P. C., Tafalla M., 1999, *ApJ*, 526, 788
 Ossenkopf V., Henning T., 1994, *A&A*, 291, 943
 Penzias A. A., 1981, *ApJ*, 249, 518
 Pickett H. M., Poynter R. L., Cohen E. A., Delitsky M. L., Muller J. C. P. H. S. P., 1998, *J. Quant. Spectrosc. & Rad. Transfer*, 60, 883
 Rawlings J. M. C., Hartquist T. W., Menten K. M., Williams D. A., 1992, *MNRAS*, 255, 471
 Rawlings J. M. C., Yates J. A., 2001, *MNRAS*, 326, 1423
 Ward-Thompson D., André P., Kirk J. M., 2002, *MNRAS*, 329, 257
 Whitworth A. P., Bate M. R., 2001, *MNRAS*, 333, 679
 Whitworth A. P., Ward-Thompson D., 2001, *ApJ*, 547, 317
 Wilson T. L., Rood R. T., 1994, *ARA&A*, 32, 191